

Four-wave mixing in strongly driven two-level systems

Witold Chałupczak, Wojciech Gawlik, and Jerzy Zachorowski

Instytut Fizyki, Uniwersytet Jagielloński, ulica Reymonta 4, 30-059 Kraków, Poland

(Received 28 September 1993)

We present experimental results of ac-Stark-effect-enhanced four-wave mixing in a dense sample of two-level atoms. The mixing efficiency exhibits strong maxima when the beams fulfill resonance and phase-matching conditions for the transitions in a dressed atom. The experimental arrangement enabled the verification of recent theories of parametric interactions in strongly driven systems. Good agreement of these theories with the experimental results allows one to use the wave mixing in the studies of properties and dynamics of strongly driven, dense, two-level systems. In particular, the possible role of parametric interaction in the phenomenon of conical emission has been analyzed in this manner.

PACS number(s): 42.65.Hw, 42.50.Hz

I. INTRODUCTION

Four-wave mixing (FWM) is one of the most important processes in nonlinear optics and has been extensively studied for media with various energy-level configurations and for various geometries of the interacting beams [1]. The effect still remains an interesting topic in view of such important applications as third-harmonic generation and phase conjugation. One of the simplest, yet most fundamental, cases is FWM in a strongly driven two-level system. Intense laser light of frequency ω_L modifies the atomic energy structure by the ac Stark effect. This modification can show up in the spectrum of resonance fluorescence, i.e., of spontaneous emission from the strongly driven (dressed) atom [2], which contains three lines known as the Mollow triplet: one at the laser frequency and the two others at the Rabi sidebands $\omega_{B,R} = \omega_L \pm \Omega'$, where $\Omega' = [(\omega_L - \omega_0)^2 + (ED/\hbar)^2]^{1/2}$, and ω_0 is the atomic frequency [3]. The properties of strongly driven atoms can also be studied in pump-probe experiments, which yield absorption spectra of the dressed atoms. These spectra also exhibit three resonant features, which appear when the frequency ω_p of the probe beam matches ω_L and/or $\omega_{B,R}$. The atom can show negative absorption (gain) on the sideband which is far from the resonance frequency, i.e., on the blue sideband ω_B for the blue-detuned laser. This can be explained as a process in which two laser photons are absorbed and a sideband photon is emitted, hence the name three-photon scattering (TPS). The probe is absorbed at the sideband which is close to ω_0 , i.e., at ω_R if $\omega_L > \omega_0$. (If $\omega_L < \omega_0$, probe absorption occurs at ω_B and gain at ω_R .) As shown in the following section, a much more intuitive explanation of these spectral features can be based on the dressed-atom model. In this model the gain on one sideband is simply due to a population inversion between the appropriate dressed-atom states, whereas absorption occurs on the other sideband as the populations of the corresponding dressed states are not inverted. The third, dispersion-shaped feature centered at $\omega_p = \omega_L$ is due to coherence of the dressed states [4]. The relative amplitudes of these features depend on the pump-laser

detuning [5], on the intensity ratio between the pump and probe beams [6], and on the relaxation rates [7]. In particular, the experiment of Carlsten, Szöke, and Raymer [8] has shown strong quenching of the gain in the three-photon effect caused by the collisional relaxation.

In addition to resonance fluorescence and absorption measurements, FWM offers a convenient way of studying the ac Stark effect in the optical domain. Harter and Boyd [9], Boyd *et al.* [10], Nilsen and Yariv [11], and Wilson-Gordon and Friedmann [12] have theoretically analyzed ac-Stark-effect-enhanced FWM in two-level systems, while Tai, Deck, and Kim [13] have performed experiments in a four-level system. We present below the results of experiments on ac-Stark-effect-enhanced FWM in dense ($N \approx 10^{14} \text{ cm}^{-3}$) samples of two-level atoms which verify existing theories of such processes. Good qualitative agreement of the experimental results with these theories enables FWM to be used as a tool for precise studies of the properties of dense ensembles of strongly driven atoms.

II. FWM IN DRESSED ATOMS

The response of an atomic ensemble driven by a strong field of amplitude E_L to a weak probe beam (amplitude E_p) can be readily calculated with the help of a density-matrix formalism along the lines of Ref. [10]. The polarization induced by the probe has its main spectral components at the probe frequency and at the mixing frequency:

$$P = P(\omega_p) + P(2\omega_L - \omega_p) + \dots \\ = \chi_{\text{TPS}} E_p + \chi_{\text{FWM}} E_L^2 E_p^* + \dots, \quad (1)$$

where χ_{TPS} and χ_{FWM} denote the dressed-atom susceptibilities associated with, respectively, the direct reaction on the probe beam and the mixing between the pump and probe discussed in Ref. [10].

The first term in Eq. (1) represents TPS and is responsible for transmission of the probe beam. The second term describes the response of the system at the mixing frequency $2\omega_L - \omega_p$, due to the FWM process. Its direction

is determined by the phase-matching condition $\mathbf{k}_{\text{FWM}} = 2\mathbf{k}_L - \mathbf{k}_p$. It should be realized that perturbation by the pumping beam at ω_L is treated to all orders in Eq. (1) while that of the probe beam is only treated in first order. This approach generalizes the standard, perturbative $\chi^{(3)}$ treatment of nonlinear optics. Such a process can be resonantly enhanced, provided that the frequency ω_p falls sufficiently close to the Rabi sideband frequencies ω_B, ω_R . The mixing amplitude is a symmetrical function of the frequency difference $\omega_p - \omega_L$. This symmetry may be broken at higher probe beam intensity, where asymmetry is caused by a frequency dependent saturation of the population inversion [12].

TPS and FWM can be conveniently described in terms of the dressed-atom model [2]. The dressed-atom states form an infinite series of doublets split by $\hbar\Omega'$, and separated by $\hbar\omega_L$ (Fig. 1). The eigenstates $|n, \pm\rangle$ are obtained by diagonalization of perturbation due to the pump field of n photons. When $\omega_L = \omega_0$, the populations of the dressed states are equal but they differ when the pump is not resonant [as shown in Figs. 1(b) and 1(c) for the considered case of $\omega_L > \omega_0$]. One of the advantages of the dressed-atom picture is that the dressed states account for the driving field to all orders. Analysis of radiative processes which involve additional weak fields can thus be reduced to consideration of transitions induced between the dressed states by these weak fields only. In particular, the TPS gain occurring when $\omega_p = \omega_B$ is related to stimulated emission resulting from population inversion between $|n+1, +\rangle$ and $|n, -\rangle$, whereas absorption occurs on the other sideband ω_R as the populations of $|n+1, -\rangle$ and $|n, +\rangle$ are not inverted [Fig. 1(b)]. On the other hand, the FWM process, i.e., generation of the $2\omega_L - \omega_p$ radiation corresponds to the cascade transitions which link two steps of the dressed-state ladder separated by $2\hbar\omega_L$ [Fig. 1(c)]. The FWM cascades involve transitions stimulated by the probe tuned to either of the sidebands accompanied by the emission on the other sideband frequency (so that $\omega_R + \omega_B = 2\omega_L$). Since in the case of FWM the cascades $\omega_R + \omega_B$ are between pairs of levels which have equal populations: $|n+1, +\rangle$ and

$|n-1, +\rangle$ as well as $|n+1, -\rangle$ and $|n-1, -\rangle$, the possible FWM gain can only be due to a parametric wave coupling. In terms of classical theory [10] this coupling is due to the mixing response described by the second term in (1) which gives rise to generation (or amplification) of the wave at frequency $2\omega_L - \omega_p$. FWM exhibits three resonance maxima: at ω_R, ω_B , and in a completely degenerate case at ω_L , while gain due to TPS occurs only at one of the sidebands.

The experimental conditions under which we have performed our study are very close to those which are necessary for observation of so-called conical emission (CE). Conical emission is a process in which strong laser light, blue detuned from the atomic transition, propagates in a relatively dense medium and produces radiation which is redshifted and emitted into a cone at a small angle to the central beam. This similarity of the experimental conditions suggests that FWM could play an important role in CE [14–16]. Boyd *et al.* [10] have shown that there is high FWM gain in strongly driven atoms at the frequencies of the Rabi sidebands. This gain is a combined effect of TPS and FWM. Any input signal on one of the sidebands produces parametric emission at the frequency of the other. It has been speculated that CE arises from such parametric FWM, seeded by a laser background. This hypothesis was supported in experiments by Harter and Boyd [14] and Plekhanov *et al.* [17] performed under conditions of self-focusing. However, as shown in our recent experiments [18, 19], CE in a weak-light-intensity regime is mainly due to cooperative spontaneous emission by a dense ensemble of strongly driven (dressed) atoms and not to parametric wave mixing.

III. EXPERIMENT

We have performed our experiment under the same conditions as our previous studies of CE. We have chosen barium vapor as the two-level, nonlinear medium and have very carefully eliminated self-trapping of the laser beams, which could severely affect the observations.

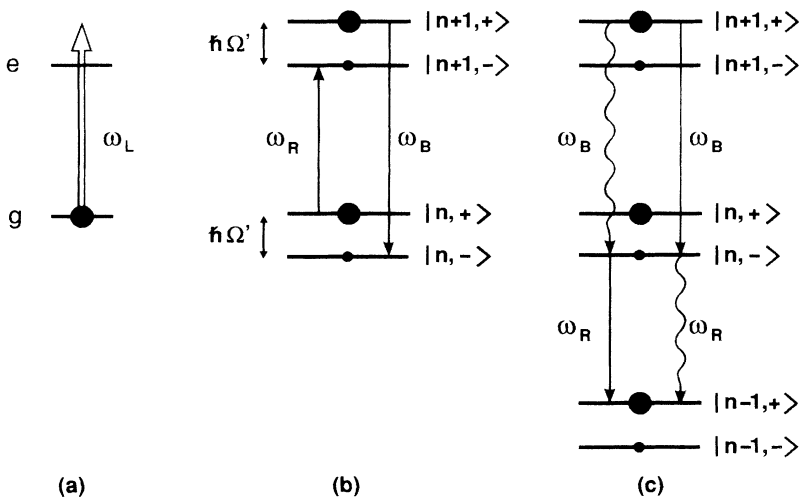


FIG. 1. Energy-level structures: (a) two-level atom perturbed by blue-detuned laser field; (b) transitions between dressed states induced by a weak probe beam tuned to the Rabi sidebands; (c) cascades $\omega_R + \omega_B$ between dressed states leading to parametric generation of the light at $2\omega_L - \omega_p$. The transitions induced by the probe are depicted by solid arrows and the parametric emission is represented by wavy arrows. The circles mark populations of the energy levels.

Self-trapping of a strong laser beam considerably modifies the refractive index of the medium thereby producing a waveguidelike channel for the propagating beam. According to Harter and Boyd [14], internal reflection and refraction on the channel walls changes the directions of the waves participating in the mixing process. Confinement of the interaction region to a narrow filament results in modification of the standard phase-matching condition so that only longitudinal components of the wave vectors are conserved [20]. In addition, because of saturation and intensity stabilization within the filament, the FWM signals do not show their characteristic intensity dependence if self-trapping occurs. It is thus crucial to eliminate self-filamentation in order to perform the experiment under clean conditions and to be to a large extent free from systematic errors.

We used two dye lasers pumped by a pulsed Nd:YAG (yttrium aluminum garnet) laser. One of the lasers (the pump) was tuned to the high-frequency side of the $6s^2^1S_0-6s6p^1P_1$ 553.548-nm transition in barium, 10–200 GHz from the line center ω_0 , whereas the frequency of the second (probe) laser was varied in a wide range around ω_0 . Both lasers emitted pulses about 10-ns long and had linewidth of about 5 GHz and energies in the range 1–70 μJ . They were weakly focused in a heat-pipe-like oven with barium vapors at about 900 °C ($N \approx 10^{14} \text{ cm}^{-3}$) and about 20 torr of argon. The pump and probe beams intersected within the cell at a small angle [Fig. 2(a)]. The light behind the cell was analyzed spectrally by a grating spectrograph with 4-GHz resolution and spatially by a charge-coupled-device camera. The beam intensities were measured with a photodiode. More experimental details are reported in Ref. [18].

IV. RESULTS AND DISCUSSION

The experiments were performed with the driving laser blue detuned ($\delta_L = \omega_L - \omega_0 > 0$). For this detuning the propagation of the pump laser beam in barium vapor is associated with CE. As shown earlier [18], the light scattered into the cone has the frequency of the red Rabi sideband [see also Fig. 3(a)]. The absence of the component at the high-frequency sideband (in the cone and in the central beam) is most likely due to strong collisional relaxation in the medium: on one hand, the spectrum of the resonance fluorescence of the collisionally perturbed dressed atoms becomes asymmetrical, i.e., for $\delta_L > 0$ the

amplitude of the high-frequency sideband becomes smaller than that of the low-frequency one, while on the other hand, collisions decrease the gain due to TPS at the high-frequency sideband.

Spatial and temporal shape of laser pulses causes some indetermination of the Rabi frequency. However, as FWM is a nonlinear process the signals are mainly determined by the peak values of the time- and position-dependent Rabi frequency and their spectra are sufficiently narrow to allow detailed analysis.

Since our interest in FWM stemmed from the studies of CE, we worked with the probe beam propagating at an angle ϑ to the pump beam close to the half angle of the light cone of CE due to the pump beam ($1^\circ-3^\circ$, depending on the particular N and δ_L values, in particular, the value of the cone angle increased when the detuning δ_L decreased). When the probe laser was tuned to the frequency of either of the Rabi sidebands, two distinct features were observed: an amplification of the probe and a new light beam, caused by FWM, emitted at complementary ($-\vartheta$) angle (Fig. 2). As can be seen in Fig. 2(b), amplification of the probe is not strictly limited to the probe beam cross section but extends into a crescentlike region surrounding the pump beam. In Fig. 3 we present spectra of the light emitted into a large solid angle behind the oven, with the central beam partly blocked by a beam stop to prevent saturation of the detector, for three different detunings of the probe beam. They indicate strong amplification when ω_p matches either the frequency of the blue sideband ω_B [Fig. 3(b)] or ω_L [Fig. 3(c)]. The amplification at ω_B can be associated with the TPS gain [7] and the one at ω_L with the Rayleigh resonance, i.e., with coherence of the dressed states [4]. As expected, there is no amplification at $\omega_p = \omega_R$ since there is no inversion of the corresponding dressed-atom populations when $\omega_L > \omega_0$. Though no quantitative analysis of the gain has been made, Figs. 3(b) and 3(c) illustrate that the Rayleigh gain is considerably bigger than the TPS gain. This is the consequence of both collisional relaxation and non-negligible intensity of the probe [6,7]. The TPS and Rayleigh amplification mechanisms were recently used for obtaining lasing in the dressed-state lasers [21].

The FWM emission into the well-defined direction $-\vartheta$ appears only for appropriate values of ϑ and frequencies ω_L and ω_p , which satisfy phase-matching condition $2\mathbf{k}_L = \mathbf{k}_p + \mathbf{k}_{\text{FWM}}$. It is noteworthy that the FWM emission at ω_B is not trapped within the central beam as it

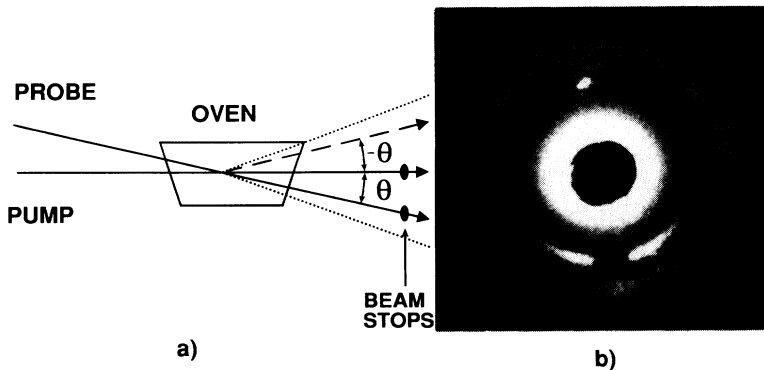


FIG. 2. (a) Experimental arrangement: dotted lines represent conical emission induced by a blue-detuned pump beam and the broken line represents the parametrically generated wave; (b) spatial light distributions behind the oven registered by a CCD camera. The development of a crescentlike structure close to the probe beam and the parametric emission into complementary angle $-\vartheta$ are observed. The black spots are due to beam stops.

should be, according to Harter and Boyd [14], in the case of self-filamentation. Additionally, sideband ω_R is emitted in our experiment under an angle $-\vartheta_C$, equal to the half angle of CE, only when the probe at ω_B is under angle ϑ_C with respect to the pump. On the other hand, in the experiment of Plekhanov *et al.* [17], performed with sodium vapor under conditions of self-focusing, the FWM emission at ω_R occurs into a cone of half angle ϑ_C when the probe at ω_B was exactly parallel to the pump. This clearly illustrates that in Ref. [17] only longitudinal components of wave vectors are conserved, $2k_L = k_B + k_R \cos \vartheta_C$, which is typical for self-focusing, whereas our FWM experiment is really not affected by self-filamentation. It should also be noted that the

nonzero value of ϑ enables the FWM signal to be easily separated from the pump and probe beams and CE making possible its precise analysis. In Fig. 4 we present spectra of the FWM beam extracted by a small diaphragm from the remaining light components. For this measurement we did not separate the FWM beam completely in order to see all the components. The spectra of Fig. 4 indicate that when ω_p is tuned to one of the Rabi sidebands, the FWM process generates directional emission of the beam that has the frequency of the other sideband. As can be seen from the excitation spectrum, i.e., the plot of the FWM beam intensity I_{FWM} versus the detuning of the probe beam $\delta_p = \omega_p - \omega_0$, presented in Fig. 5, FWM depends resonantly on detuning of the probe

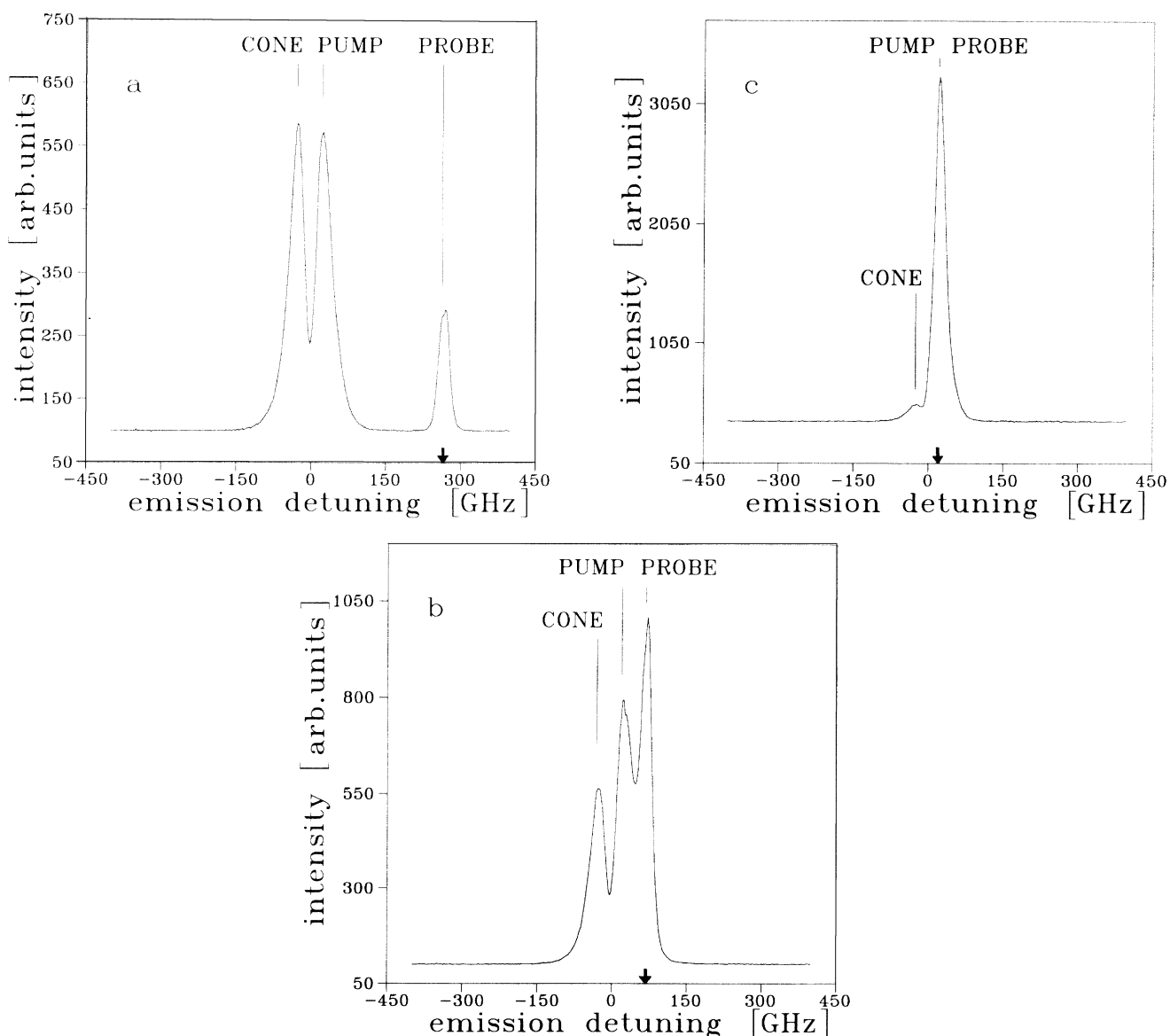


FIG. 3. Emission spectra behind the oven for various probe detunings: (a) when ω_p is far from resonance with ω_0 and ω_L , one observes a characteristic, two component spectrum of conical emission and pump-laser beam and a signature of a passively transmitted probe beam; (b) when $\omega_p = \omega_B$, the probe is amplified by TPS; (c) when $\omega_p = \omega_L$, a very strong Rayleigh gain occurs. Different intensity scales reflect differences in absolute intensities of the spectra. Vertical arrows mark ω_p . Emission detuning is with respect to ω_0 .

from the Rabi sidebands. This is a clear manifestation of ac Stark enhancement. The maximum values of I_{FWM} at resonance increase when the pump beam detuning δ_L is decreased.

Theoretical considerations [9,10] predict full symmetry of both resonances in Fig. 5. In our experiment, however, some asymmetry is evident. The asymmetry could, in principle, arise from the fact that one of the FWM resonances is additionally enhanced by the TPS contribution,

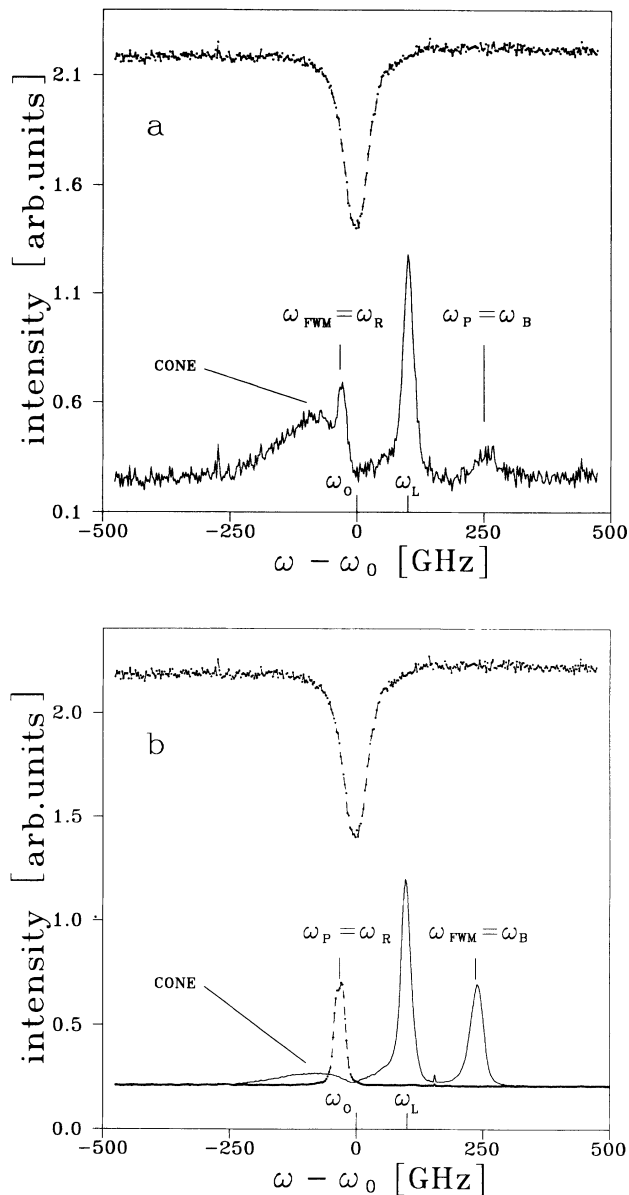


FIG. 4. Spectra of the four-wave-mixing signals for various frequencies of the probe: (a) $\omega_p = \omega_B$; (b) $\omega_p = \omega_R$. Upper traces show linear absorption spectra. In addition to the FWM signals the contributions due to the pump and conical emission can also be recognized. In (a) the probe beam was not completely blocked so its signature is seen at ω_p . In (b) the FWM emission was better selected and the probe contribution (broken line) was extra determined for frequency reference. Detunings are with respect to ω_0 .

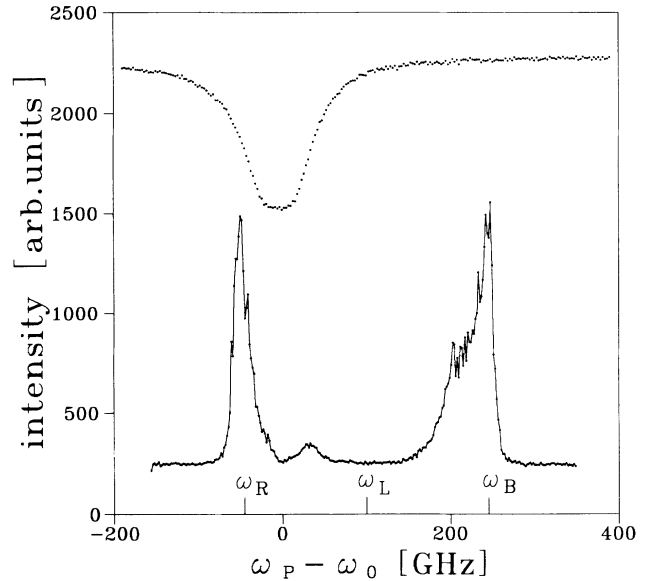


FIG. 5. Four-wave-mixing signal intensity as a function of the probe beam detuning. Upper trace is the linear absorption spectrum for frequency reference. Pump beam energy is $8 \mu\text{J}$, probe beam energy is $12 \mu\text{J}$.

but as noted above, TPS gain is small in our case because of collisional damping. Most importantly, the asymmetry is due to reabsorption effects that occur during propagation of the beams both before and behind the intersection, i.e., in the nonpumped area. Such reabsorption, which has not been included in theory, manifests itself by a dip at ω_0 in the spectra of Fig. 5. Small distortion of the signal due to reabsorption of the signal beam can also be seen in the second maximum. In addition to the maxima at the Rabi sidebands seen in Fig. 5, the theory predicts another resonance in the $I_{\text{FWM}}(\delta_p)$ dependence, associated with the Rayleigh resonance at

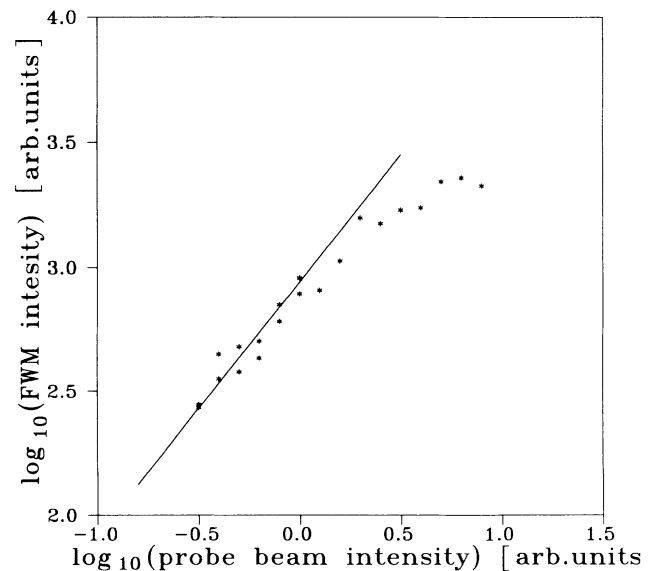


FIG. 6. Four-wave-mixing signal intensity vs the probe beam intensity for $\omega_p = \omega_R$, pump beam intensity is $32 \mu\text{J}$, maximum probe beam intensity is $18 \mu\text{J}$.

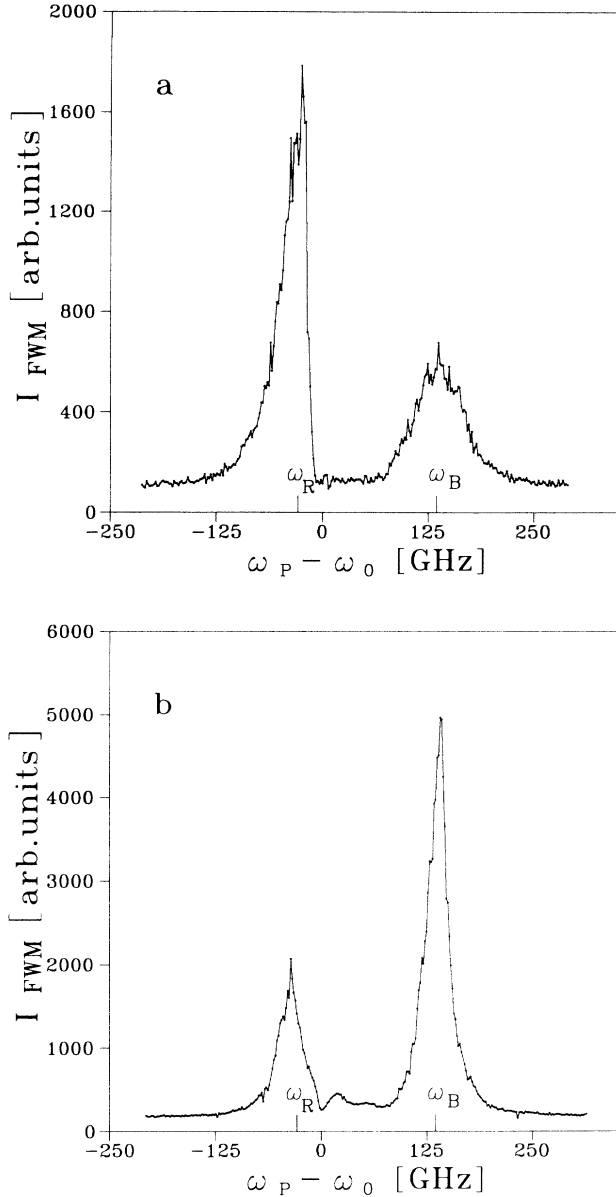


FIG. 7. Excitation spectra of the four-wave-mixing signal for pump beam energy $I_L = 7 \mu\text{J}$ and probe laser energies (a) $7 \mu\text{J}$ and (b) $70 \mu\text{J}$.

$\omega_p = \omega_L$ (degenerate FWM). This resonance cannot be detected in the geometry of our experiment as a new spatially separated feature.

We have verified that for weak probe beams the amplitude of the FWM signal is a linear function of the probe intensity, in agreement with Eq. (1). At higher probe-beam intensities, however, the FWM signals could be affected by additional saturation effects due to the strong probe as seen in Fig. 6. The study of the effects caused by

two strong beams requires calculations which go beyond those leading to Eq. (1). Such calculations have recently been performed by Wilson-Gordon and Friedmann [12]. They predict asymmetry of the $I_{\text{FWM}}(\delta_p)$ spectra because the saturation with the increase of the probe beam intensity is stronger for the sideband that is closer to ω_0 . This prediction is very well confirmed by our measurements. In Fig. 7 we present the excitation spectra taken with weak ($7 \mu\text{J}$) and strong ($70 \mu\text{J}$) probe beams which demonstrate the saturation behavior.

V. CONCLUSIONS

We have performed systematic studies of ac-Stark-enhanced FWM in a dense ensemble of two-level atoms. Due to the elimination of self-trapping and because of the easy discrimination of the mixing signal (spatial separation) we have obtained results that enable a reliable comparison with theoretical calculations to be made. Our results confirm the main predictions of earlier theoretical models [10,12]. In particular, we have verified that FWM is very efficient when the probe beam is resonant with the energy-level structure of the dressed atoms and that the excitation spectrum of FWM depends significantly on the intensities of both light beams. We have also clarified the extent to which the FWM process can affect the phenomenon of CE and have found that in the low-intensity and no-self-focusing regimes these are in fact quite distinct phenomena. In this conclusion we differ from Harter and Boyd [14] as well as from Plekhanov *et al.* [17], who performed probe-beam studies of a possible role of FWM in CE. We think that this discrepancy results from the fact that in Refs. [14] and [17] self-focusing was seriously affecting the experimental results. Moreover, the authors of [14] and [17] worked with sodium which has more complicated energy-level structure than barium which can be treated as a two-level system.

Some possible applications of these results have already been pointed out, including tunable light harmonic generation [13], beam coupling [6], and phase conjugation [9,11]. In addition, we believe that measurements of the kind reported here could yield valuable information about the actual Rabi frequencies in dense atomic systems where collective atomic effects are responsible for differences between the local and external fields [22]. Very interesting related problems are also inversionless amplification [23] and energy transfer [6] between light beams due to FWM.

ACKNOWLEDGMENTS

This work has been supported in part by the Polish Committee for Scientific Research (Grant Nos. 201139101 and 2 P30205205). We are grateful to R. W. Boyd for discussions and to S. Lea for critical reading of the manuscript.

[1] Y. R. Shen, *The Principles of Nonlinear Optics* (Wiley, New York, 1984).

[2] C. Cohen-Tannoudji, J. Dupont-Roc, and G. Grynberg, *Atom-Photon Interactions* (Wiley, New York, 1992).

[3] B. R. Mollow, *Phys. Rev.* **188**, 1969 (1969).

[4] N. Lu and P. R. Berman, *Phys. Rev. A* **44**, 5965 (1991).

[5] F. Y. Wu, S. Ezekiel, M. Ducloy, and B. R. Mollow, *Phys. Rev. Lett.* **38**, 1077 (1977).

- [6] M. T. Gruneisen, K. R. MacDonald, A. L. Gaeta, and R. W. Boyd, *Phys. Rev. A* **40**, 3464 (1989).
- [7] M. T. Gruneisen, K. R. MacDonald, and R. W. Boyd, *J. Opt. Soc. Am. B* **5**, 123 (1988).
- [8] J. L. Carlsten, A. Szöke, and M. G. Raymer, *Phys. Rev. A* **15**, 1029 (1977).
- [9] D. J. Harter and R. W. Boyd, *IEEE J. Quantum Electron.* **QE-16**, 1126 (1980).
- [10] R. W. Boyd, M. G. Raymer, P. Narum, and D. J. Harter, *Phys. Rev. A* **24**, 411 (1981).
- [11] J. Nilsen and A. Yariv, *IEEE J. Quantum Electron.* **QE-18**, 1947 (1982).
- [12] A. D. Wilson-Gordon and H. Friedmann, *Phys. Rev. A* **38**, 4087 (1989).
- [13] Chen-Yu Tai, R. T. Deck, and Ch. Kim, *Phys. Rev. A* **37**, 163 (1988).
- [14] D. J. Harter and R. W. Boyd, *Phys. Rev. A* **29**, 739 (1984).
- [15] Y. Shevy and M. Rosenbluh, *J. Opt. Soc. Am. B* **5**, 116 (1988).
- [16] J. F. Valley, G. Khitrova, H. M. Gibbs, J. W. Grantham, and Xu Jianjin, *Phys. Rev. Lett.* **64**, 2362 (1990).
- [17] A. I. Plekhanov, S. G. Rautian, V. P. Safonov, and B. M. Chernobrod, *Zh. Eksp. Teor. Fiz.* **88**, 426 (1985) [*Sov. Phys. JETP* **61**, 249 (1985)].
- [18] W. Chałupczak, W. Gawlik, and J. Zachorowski, *Opt. Commun.* **99**, 49 (1993).
- [19] W. Chałupczak, W. Gawlik, and J. Zachorowski, *Phys. Rev. A* **49**, R2227 (1984).
- [20] C. A. Sacchi, C. H. Townes, and J. R. Lifshitz, *Phys. Rev.* **174**, 439 (1968).
- [21] I. S. Zeilikovich, S. A. Pul'kin, and L. S. Gaida, *Opt. Spectrosk.* **62**, 1401 (1987) [*Opt. Spectrosc. (USSR)* **62**, 827 (1987)]; G. Khitrova, J. F. Valley, and H. M. Gibbs, *Phys. Rev. Lett.* **60**, 1126 (1988); A. Lezama, Y. Zhu, M. Kanskar, and T. W. Mossberg, *Phys. Rev. A* **41**, 1576 (1990); D. Grandclément, G. Grynberg, and M. Pinard, *Phys. Rev. Lett.* **59**, 40 (1987).
- [22] Ch. M. Bowden and J. P. Dowling, *Phys. Rev. A* **47**, 1247 (1993); J. P. Dowling and Ch. M. Bowden, *Phys. Rev. Lett.* **70**, 1421 (1993); J. J. Maki, M. S. Malcuit, J. E. Sipe, and R. W. Boyd, *ibid.* **67**, 972 (1991); V. V. Vasilev, V. S. Egorov, and I. A. Chekhonin, *Opt. Spectrosk.* **70**, 897 (1991) [*Opt. Spectrosc.* **70**, 525 (1991)]; M. G. Raizen, R. J. Thompson, R. J. Brecha, H. J. Kimble, and H. J. Carmichael, *Phys. Rev. Lett.* **63**, 240 (1989).
- [23] O. Kocharovskaya, *Phys. Rep.* **219**, 175 (1992); M. O. Scully, *ibid.* **219**, 191 (1992); W. Gawlik, *Comments At. Mol. Phys.* **29**, 189 (1993), and references therein.

